**Smart Structures and Systems**, *Vol. 12, No. 6 (2013) 661-678*
DOI:http://dx.doi.org/10.12989/sss.2013.12.6.661 

# Bridge load testing and rating: a case study through wireless sensing technology

Samir N. Shoukry*[1], Yan Luo[2], Mourad Y. Riad[3] and Gergis W. William[3]

[1]*Department of Mechanical and Aerospace Eng., West Virginia University, Morgantown, WV 26506, USA*
[2]*DEI Group, Millersville, MD 21108, USA*
[3]*Department of Civil and Environmental Eng., West Virginia University, Morgantown, WV 26506, USA*

*(Received February 28, 2012, Revised June 23, 2013, Accepted June 27, 2013)*

**Abstract.** In this paper, a wireless sensing system for structural field evaluation and rating of bridges is presented. The system uses a wireless platform integrated with traditional analogue sensors including strain gages and accelerometers along with the operating software. A wireless vehicle position indicator is developed using a tri-axial accelerometer node that is mounted on the test vehicle, and was used for identifying the moving truck position during load testing. The developed software is capable of calculating the theoretical bridge rating factors based on AASHTO Load and Resistance Factor Rating specifications, and automatically produces the field adjustment factor through load testing data. The sensing system along with its application in bridge deck rating was successfully demonstrated on the Evansville Bridge in West Virginia. A finite element model was conducted for the test bridge, and was used to calculate the load distribution factors of the bridge deck after verifying its results using field data. A confirmation field test was conducted on the same bridge and its results varied by only 3% from the first test. The proposed wireless sensing system proved to be a reliable tool that overcomes multiple drawbacks of conventional wired sensing platforms designed for structural load evaluation of bridges.

**Keywords:** testing and inspecting procedures; bridge load rating; remote sensing; wireless data acquisition; finite element modeling

## 1. Introduction

Bridges are critical elements of the roadway system and are considered to be vital assets for the economy and security of any nation. Due to deteriorating materials, maintenance limitations, and continuously increasing load spectra, the conditions of most bridges are in a continuing decline. For this reason, evaluating the actual structural capacity of deteriorating bridges is becoming increasingly important. Most bridges are evaluated through subjective visual inspection procedures and conservative theoretical ratings (Chajes *et al*. 1997, Chase 2001). Diagnostic load testing has been recognized as an effective method to accurately assess the carrying capacity of bridges (Phares *et al*. 2003). Bridge load testing with traditional wired data acquisition (DAQ) systems suffers drawbacks of being labor intensive, costly, and time consuming in both sensor installation

*Corresponding author, Dr., E-mail: snshoukry@mail.wvu.edu


http://www.techno-press.org/?journal=sss&subpage=8 ISSN: 1738-1584 (Print), 1738-1991 (Online)

as well as testing procedures. For those reasons, only limited numbers of full scale load tests are conducted on bridges.

Wireless sensing technology has been identified as one of the most important technologies for the 21st century (Chong and Kumar 2003). In testing large structures, Wireless DAQ systems bring remarkable advantages because of their ease and fast installation, and savings in cost and maintenance of cables (Jo *et al*. 2013, Kim *et al*. 2013, Yuan *et al*. 2013, Hoover *et al*. 2012, Flouri *et al*. 2012, Ni *et al*. 2011, Lin *et al*. 2010). The structural engineering field has begun to consider such wireless systems as substitutes for traditional wired ones (Lynch and Loh 2006). After Straser and Kiremidjian (1998) presented a low-cost wireless monitoring system for civil structures, a number of research teams in both the academic and industrial fields have proposed a few wireless sensor prototypes featuring a wide offering of functionalities (Lynch and Loh 2006). As the objective-based bridge load rating is getting more important and necessary for assessment of bridge capacity and for health monitoring, the wireless sensing technology has an enormous potential in this area.

## 2. Wireless sensory system for bridge load testing

For conducting a bridge load test, the following bridge responses are commonly required at critical elements: strains, displacements, rotations, and dynamic characteristics (Lichtenstein 1998). For the specific calculations of bridge rating factors according to AASHTO Load Resistance Factor Rating (LRFR) procedures, strain values are the essential records while other measurements are complimentary.

The suggested wireless DAQ system for bridge load testing was developed based on the MicroStrain® wireless sensing platform. The wireless DAQ system includes wireless strain sensors, wireless accelerometers and a novel wireless vehicle position indicator for monitoring truck position during load testing. With the capability of high-speed data acquisition simultaneously for multiple wireless sensors, the MicroStrain wireless sensing platform includes a USB wireless antenna, wireless nodes for different applications, and software. The wireless nodes utilize IEEE 802.15.4 Direct Sequence Spread Spectrum (DSSS) and work at 2.4 GHz radio frequency with a communication range up to 300 m. Equipped with a 12-bit A/D convector and a 2 MB on-board memory, the nodes can stream at 4 KHz and datalog at 2 KHz sampling rate. The wireless nodes used in this research are V-Link® voltage nodes, SG-Link® strain nodes, and G-Link® accelerometer nodes.

Three main sensing blocks are integrated for the wireless bridge load testing system; (1) wireless strain sensors, (2) wireless accelerometers and (3) wireless vehicle positioning indicator (WVPI). The V-Link node manufactured by Microstrain has four differential channels that allow connecting with strain sensors. Quarter-bridge strain gages 350 Ω manufactured by OMEGA were integrated with the V-Link node through external bridge completion modules. Seismic force-balanced accelerometers manufactured by Columbia Research Laboratories are integrated with the SG-Link node. The accelerometer ranges from DC level to 100 Hz, with a capacity of ±0.5G and a sensitivity of 10V/G. Because the voltage input range of the wireless node is 0 to 3 V, a signal conditioning board and a power supply were necessary for the accelerometer. The G-Link nodes have internal microelectromechanical system (MEMS) capacitive accelerometers. The wireless vehicle positioning indicator used a G-Link node by mounting it on the loading truck wheel hub to measure its rotating angle. The rotation of the wheel is related to the linear position

of the wheel, namely the position of the truck. With the advantage of wireless transmission, compact and light-weight measuring only 46 grams, the G-Link node becomes an ideal device to monitor the position of a test truck for bridge load testing. Fig. 1 shows the Hardware main sensing blocks, while Fig. 2 illustrates a schematic diagram of the suggested wireless bridge load testing and rating system. Wireless strain sensors and wireless accelerometers are mounted on bridge girders to measure strain and vibration responses. Once the wireless nodes receive the triggering command, they automatically start to collect and save signals simultaneously. Recorded data are wirelessly downloaded to the laptop at the site and are then processed using the developed software to calculate the rating factors ($RF_T$).

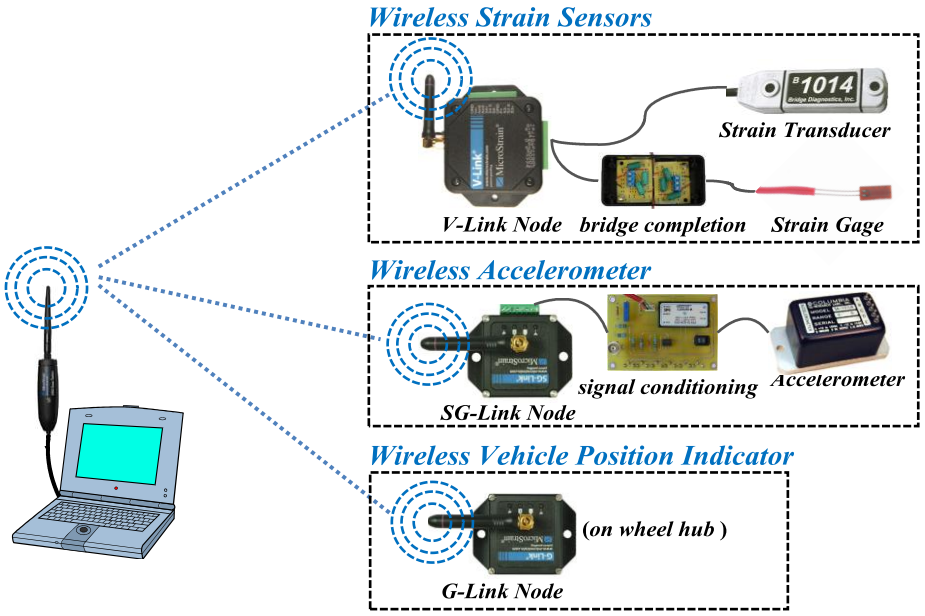


Fig. 1 Hardware sensing blocks of wireless bridge load testing system

## 3. Wireless vehicle position indicator (WVPI)

The WVPI uses a G-Link wireless accelerometer node with ±2 g range, manufactured by MicrosStrain. The wireless node is powered by an internal rechargeable battery (180 mAhr) with very low power consumption (0.18 mA in the sleeping mode, 15 mA for the datalogging mode). It works on 2.4 GHz radio frequency with 70 m line-of-sight communication range, featuring 2 KHz sampling rates, combined with 2 MB onboard flash memory for data storage. The node integrates two orthogonally, dual- axis MEMS capacitive accelerometers. The accelerometer outputs acceleration signals in *x*, *y* and *z* axes respectively. This triaxial accelerometer is used as a tilt sensor to measure the inclination or angle of change with respect to gravity. It can be used to measure a full 360°of orientation through gravity by using two accelerometers oriented perpendicular to one another. The accelerometer is most sensitive to tilt when its sensitive axis is perpendicular to the force of gravity. At this orientation, its sensitivity to changes in tilt is highest.

When the accelerometer is oriented on axis to gravity, the change in output acceleration per degree of tilt is negligible. When one sensor is reading a maximum change in output per degree, the other is at its minimum. The output tilts in degrees of *x*- and *y*-axis (xRoll and yRoll respectively) are calculated by Eqs. (1) and (2)

$$xRoll = ASIN\left(\frac{Ax}{1g}\right) \tag{1}$$

$$yRoll = ACOS(\frac{Ay}{1g}) \tag{2}$$

Where *Ax* and *Ay* are measured accelerations in the x and y axes respectively.

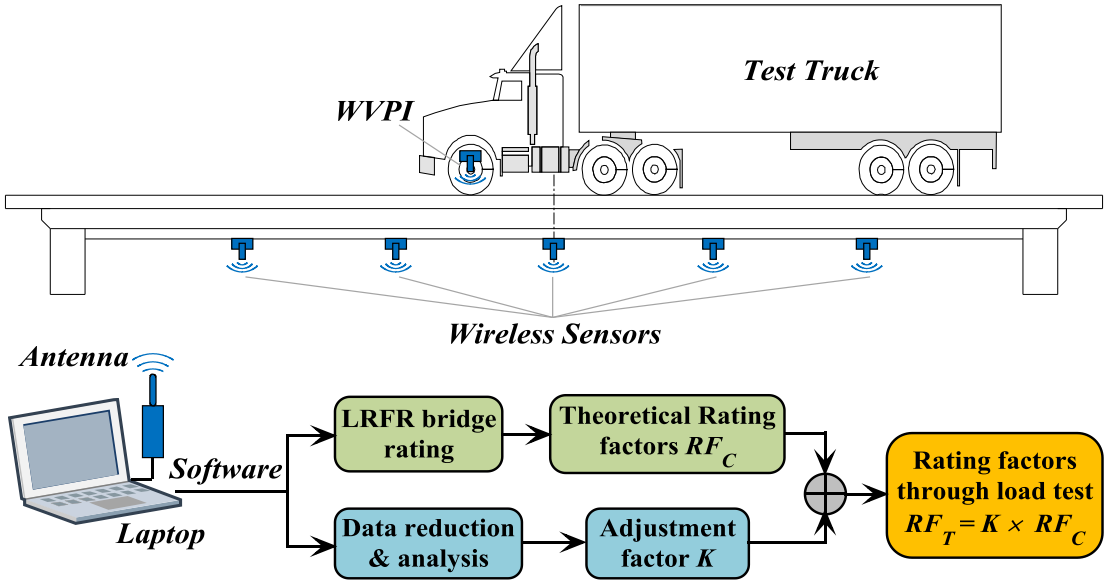


Fig. 2 Schematic diagram showing the wireless sensory system and post processing blocks

Interpretation of Eqs. (1) and (2) are shown in Fig. 3. By mounting the G-Link wireless node on the wheel hub of the test truck, it is possible to monitor the rotation of the wheel by identifying the acceleration peaks and valleys. In every cycle, those peaks and valleys correspond to rotating angles of 0°, 90°, 180°, and 270° respectively. By combining the time coordinates of peaks & valleys with the wheel circumference that can be easily measured, the longitudinal position of the wheel can be calculated. Thus, the linear position of the moving vehicle can be easily located based on a starting reference point. The resolution of this approach is ¼ the wheel circumference (WC) compared to one WC only if measurements were conducted using the BDI AutoClicker (Phares *et al*. 2003).An even higher resolution can be obtained with the VWPI by interpolating between those identified points assuming theoretically a sinusoidal shape of the relation between the rotation angle and acceleration (Luo 2010).

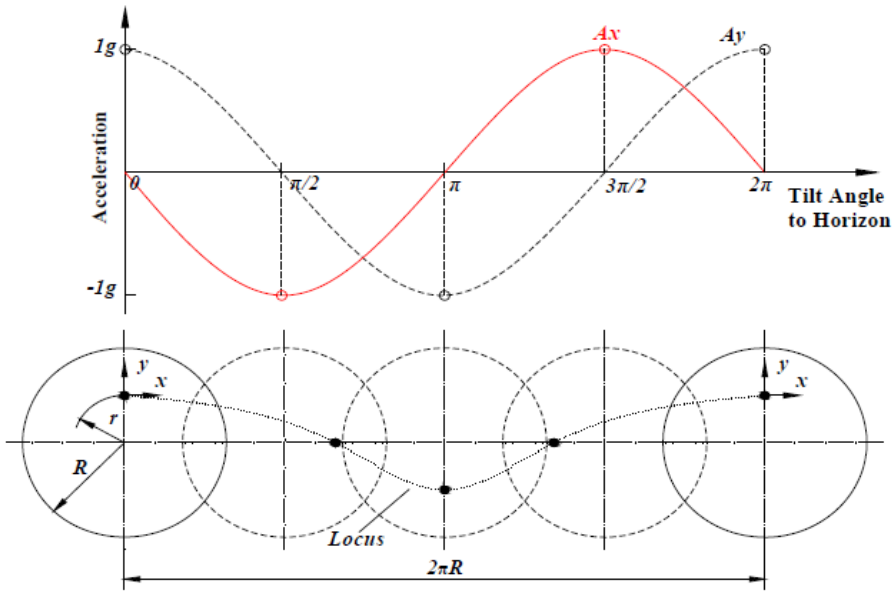


Fig. 3 Relationship between tilt angle and acceleration

Assuming the value array of peaks & valleys obtained from the WVPI signals is $PV = \{pv_1, pv_2, \cdots, pv_n\}$, and the corresponding time array is $T = \{t_1, t_2, \cdots, t_n\}$. The initial angle α of the first peak or valley can be calculated from the ratio of its magnitude to peak-to-peak value:

$$\alpha = \sin^{-1}\left(\frac{|pv_1|}{|pv_2 - pv_1|/2}\right) \tag{3}$$

Then, the array of vehicle positions $POS = \{pos_1, pos_2, \cdots, pos_n\}$ corresponding to $T = \{t_1, t_2, \cdots, t_n\}$ can be presented as

$$pos_i = \frac{\alpha \times WC}{2\pi} + \frac{WC}{4} \times (i-1), \ (i = 1,2,\cdots,n) \tag{4}$$

Recorded signals coming from a moving vehicle are normally noisy because of the vibration of the engine and due to the excitation from the rough roads. The 1-D double-density complex digital wavelet transform (DWT) denoising algorithm is used to denoise the recorded signals. The Double-density complex (or double-density dual-tree) DWT is based on the combination of double-density DWT and dual-tree DWT, because these two DWTs have their own distinct characteristics and advantages. In order to combine the properties of both the double-density and dual-tree DWTs, the following conditions are implemented: (1) one pair of wavelets is designed to be offset from the other pair so that the integer translates of one wavelet pair fall midway between the integer translates of the other pair, and (2) one wavelet pair is designed to be approximate Hilbert transforms of the other pair (Selesnick 2004). This algorithm possesses good directional

selectivity and can be used to implement complex and directional wavelet transforms in multiple dimensions. The denoising algorithm proved to be very effective in this application as can be seen in the WVPI signal example given in Fig. 4. By coordinating the peaks & valleys with the time, the truck positions in time domain can be identified. Local maxima and minima (peaks and valleys) in the denoised signal are found by comparing each data point to its neighboring values. A local peak is returned when its value is larger than both its neighbors while the opposite is true for valleys. Fig. 5 illustrates a sample data and analysis of truck position using the WVPI method while conducting a field test.

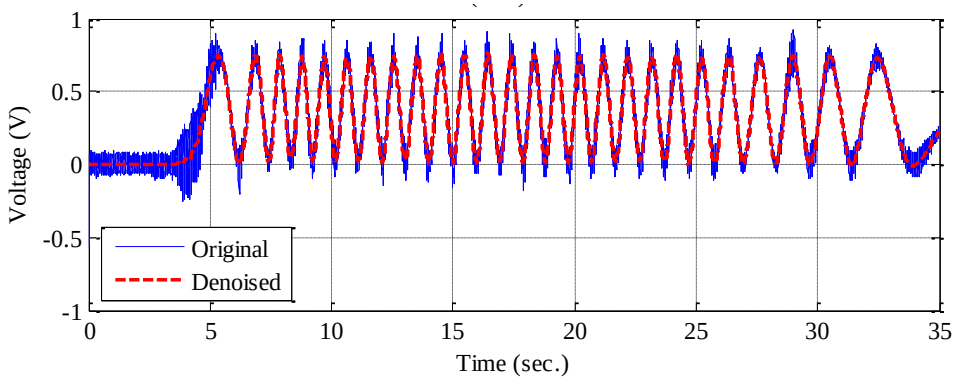


Fig. 4 Original versus denoised signal for x axis of WVPI sensor

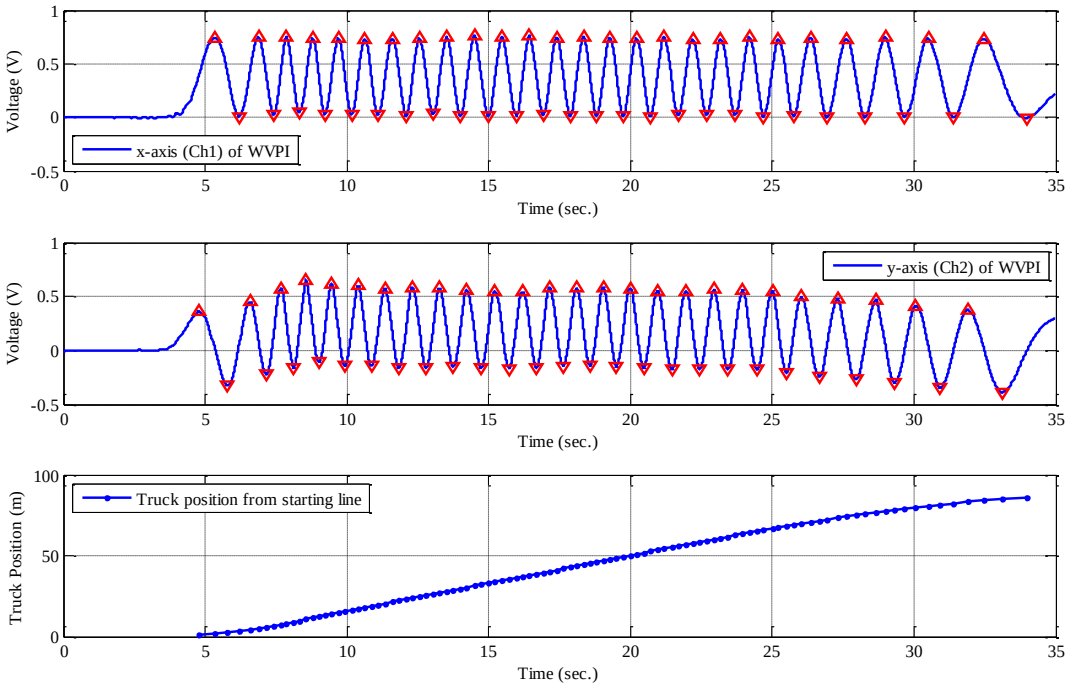


Fig. 5 Identifying truck position from a reference point using Wireless vehicle position indicator

## 4. Software package and rating according to LRFR

In 2001, the American Association of State Highway and Transportation Officials (AASHTO) developed the Load and Resistance Factor Rating (LRFR) procedures for rating bridges. The Manual for Condition Evaluation and Load and Resistance Factor Rating of Highway Bridges reflects the latest technologies on the structural reliability approach inherent in specifications for load and resistance factor design (LRFD). Before conducting the field test, full theoretical rating for the bridge superstructure is performed. The specifications in LRFR bridge rating contain three procedures; (1) design load rating, (2) legal load rating, and (3) permit load rating. In the LRFR manual, a rating factor for each component and connection subjected to a force effect is determined using the following relation

$$RF = \frac{C - (\gamma_{DC})(DC) - (\gamma_{DW})(DW) \pm (\gamma_P)(P)}{(\gamma_L)(LL + IM)} \tag{5}$$

where: $RF$ = Rating factor
$C$ = Capacity
$R_n$ = Nominal member resistance
$DC$ = Dead-load effect due to structural components and attachments
$DW$ = Dead-load effect due to wearing surface and utilities
$P$ = Permanent loads other than dead loads
$LL$ = Live-load effect
$IM$ = Dynamic load allowance
$\gamma_{DC}$ = LRFD load factor for structural components and attachments
$\gamma_{DW}$ = LRFD load factor for wearing surfaces and utilities
$\gamma_P$ = LRFD load factor for permanent loads other than dead loads
$\gamma_L$ = Evaluation live-load factor
$\varphi_c$ = Condition factor
$\varphi_s$ = System factor
$\varphi$ = LRFD resistance factor
$C = \varphi_c \varphi_s \varphi R_n$, for the Strength Limit States where $\varphi_c \varphi_s \geq 0.85$
$C = f_R$ for the Service Limit States
$f_R$ = Allowable stress specified in the LRFD specifications

The AASHTO LRFR procedures of bridge load rating through load testing are summarized in the flow chart shown in Fig. 6. Input variables are obtained from bridge inspection results, along with geometrical and material properties of the bridge elements, load configuration values (design load, legal load and permit load) etc...These procedures provide the theoretical rating factor $RF_C$. In order to optimize the process of collecting field data through instrumentation, finite element modeling studies may be conducted to calculate the moments under moving loads and obtain the critical locations on the bridge. Instrumentation plan for diagnostic load test are to be worked out according to these critical positions. Strain responses under moving loads at crawl speeds are

measured in the diagnostic load test. A comparison between measured strains and calculated ones will produce an adjustment factor *K*. The rating factors $RF_T$ through load test can then be calculated.

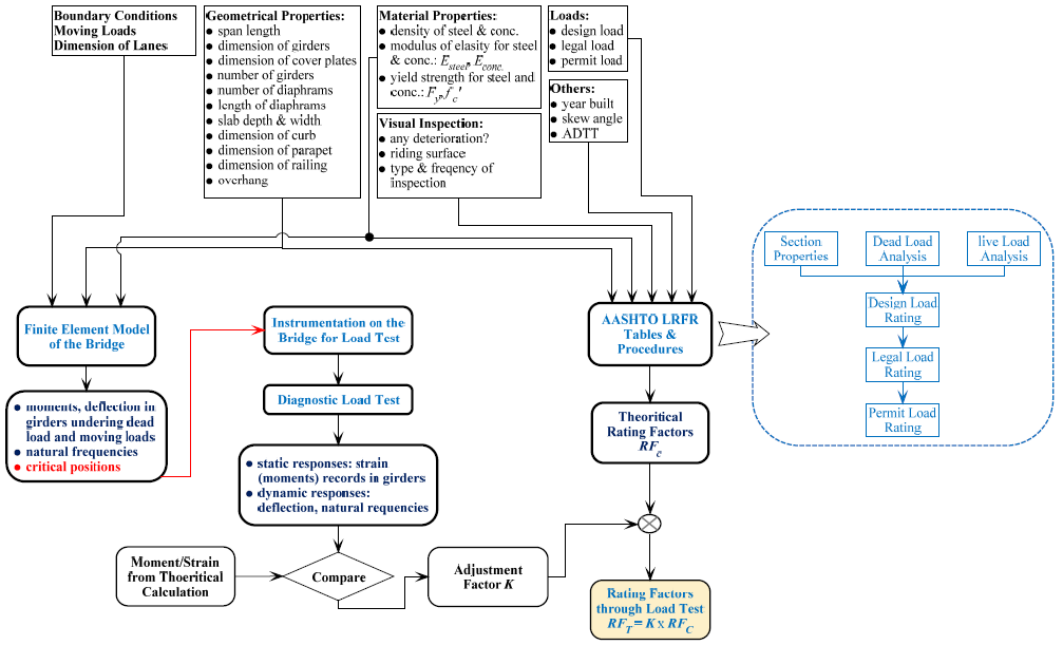


Fig. 6 Flowchart describing bridge load rating through load testing

A rating software according to the LRFR manual has been developed in Matlab code. Input data consisted of geometric dimension of various bridge elements, material properties, factors according to bridge condition, and factors related to loading and average daily traffic. Based on LRFR calculations, the software outputs the theoretical rating factor $RF_C$ automatically. In this study, the Evansville Bridge in West Virginia was selected as a test bridge for deployment of the proposed sensory system. The Evansville Bridge is designed according to the AASHTO LRFD specifications for HL-93 live load and was constructed in 2003. The bridge is located near the intersection of WV Route 92 with Route 50 over the Little Sandy Creek in Preston County, West Virginia. The bridge is a typical three-span continuous steel girder bridge with a 55° skewed angle and span lengths of 14.78, 15.24, 14.78 m respectively. The bridge is supported over two piers and two integral abutments as shown in Figure 7. The deck accommodates two traffic lanes, each 3.65 m wide, and two shoulders of widths 2.6 and 2.9 m. The bridge superstructure consists of a reinforced concrete deck 0.2 m thick supported by 7 steel girders.

Table 1 shows the theoretical rating output for the Evansville Bridge. After producing $RF_C$ according to LRFR codes, the software automatically produces the adjustment factor *K* based on load testing data to obtain field rating factors $RF_T$ where

$$RF_T = K \times RF_C \tag{6}$$

The adjustment factor ($K$) is given by

$$K = 1 + K_a \times K_b \tag{7}$$

The factor $K_b$ has values between 0 and 1 and is determined according to tables in the LRFR, indicating the level of test benefit that is expected at the rating load level. The factor $K_a$ accounts for the section factor and is determined by

$$K_a = \left(\varepsilon_C / \varepsilon_T\right) - 1 \tag{8}$$

where: $\varepsilon_T$ = maximum member strain measured during load test.

$\varepsilon_C$ = Corresponding calculated strain due to the test vehicle, at its position on the bridge which produced $\varepsilon_T$ .

## 5. Validation of the wireless DAQ system

In order to assess the performance of the wireless sensors and data acquisition system prior to deployment on the bridge site, wireless sensors were tested alongside with their wired counterparts. Comparing test results from both systems offered a useful tool to assess the sensitivity and accuracy of the wireless DAQ system. Two strain gages were mounted in parallel at the fixed end of a cantilever beam. One strain gage was connected to the wireless node through an external quarter-bridge completion module while the other was connected to a Vishay strain recorder. Only bending moment was applied to the beam. A sample of the synchronized records acquired by wired and wireless DAQ systems is shown in Figure 8. As illustrated, the strain response measured by the wireless acquisition system matches perfectly with that measured independently by the cable-based data acquisition system.

Table 1 Theoretical rating values of the Interior Girder in Evansville Bridge Superstructure

| Limit State | | Design Load Rating | | Legal Load Rating | | | Permit Load Rating |
|---|---|---|---|---|---|---|---|
| | | Inventory | Operating | T3 | T3S2 | T3-3 | |
| Strength I | Flexure | 2.13 | 2.76 | 3.91 | 4.31 | 4.60 | -- |
| | Shear | 2.30 | 2.98 | 4.38 | 4.06 | 4.30 | -- |
| Strength II | Flexure | -- | -- | -- | -- | -- | 3.41 |
| | Shear | -- | -- | -- | -- | -- | 2.90 |
| Service II | | 1.91 | 2.48 | 3.31 | 3.65 | 3.89 | 2.61 |
| Safe Load Capacity (tons) | | -- | -- | 82.6 | 131.4 | 156.0 | -- |

In order to validate the wireless measurements of the accelerometers, two force-balanced accelerometers were installed in parallel on one of the bridge girders. One accelerometer was connected with a wireless node via a signal conditioning board, and the other one was wired with a cable-based USB DAQ device manufactured by National Instruments. Acceleration signals were

recorded while normal traffic was crossing the bridge. As illustrated in Fig. 8, comparing the time-history responses from both the wired and wireless systems indicates that the wireless DAQ system was capable of recording accurate acceleration response of the bridge under dynamic loads.

It can also be seen that the FFT spectrums from wired and wireless signals match perfectly with one another. From the frequency domain output, two obvious peaks were identified at 8.00 Hz and 10.86 Hz.

(a) Evansville Bridge

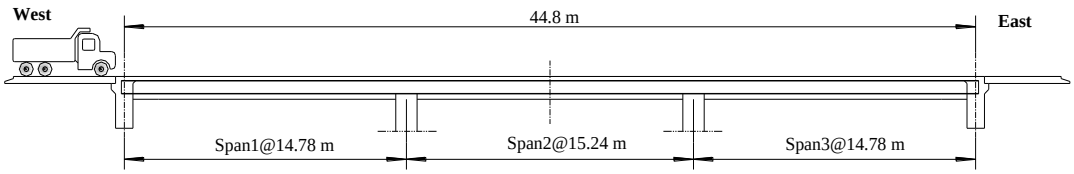


(b) Bridge Elevation

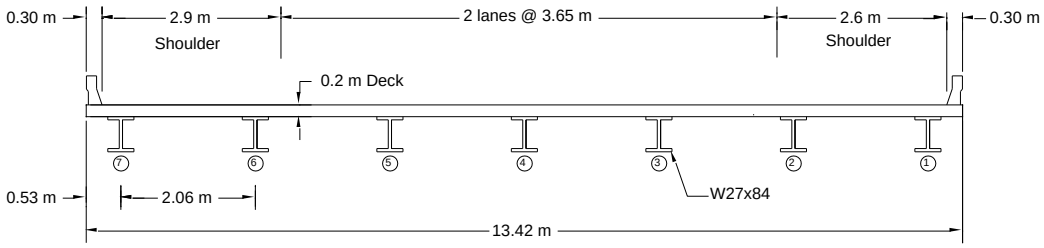


(c) Superstructure Cross Section

Fig. 7 Evansville Bridge Details

## 6. Field load test

Bridge load testing is to measure the response of critical bridge elements under controlled and predetermined loadings without causing inelastic response changes in the structure. Load tests are carried out to provide a realistic evaluation of the structure and to verify the theoretical load rating according to the LRFR Manual. It is recognized as the only way to determine the real capacity of bridges (Washer and Fuchs 1998). In this application, a diagnostic load test was carried out on the

Evansville Bridge in West Virginia. The wireless sensory system was deployed on the bridge deck while a pre-weighed dump truck was used for the moving load. Static and dynamic tests were executed and test data were analyzed and post-processed to provide a bridge rating factor. Since all sensors were installed underneath the bridge deck, the bridge was open to traffic during the entire operation. Installation of all sensors and equipments took about 3 hours and only 2 operators to conduct the test.

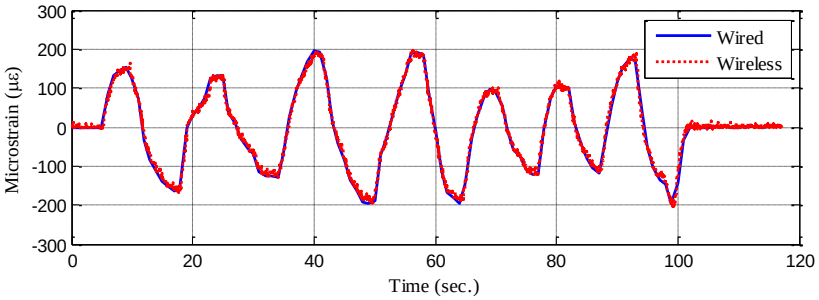


(a) Comparison of bending strains recorded by wired versus wireless systems

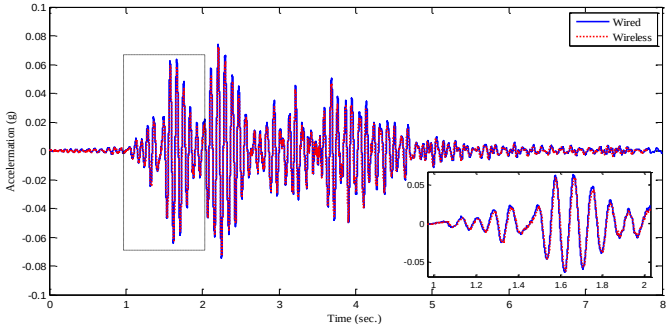


(b) Acceleration response in time domain

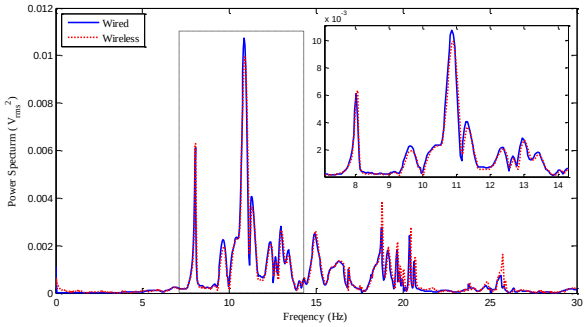


(c) Comparison of wireless and wired acceleration response in frequency domain

Fig. 8 Validation test of Wireless DAQ system

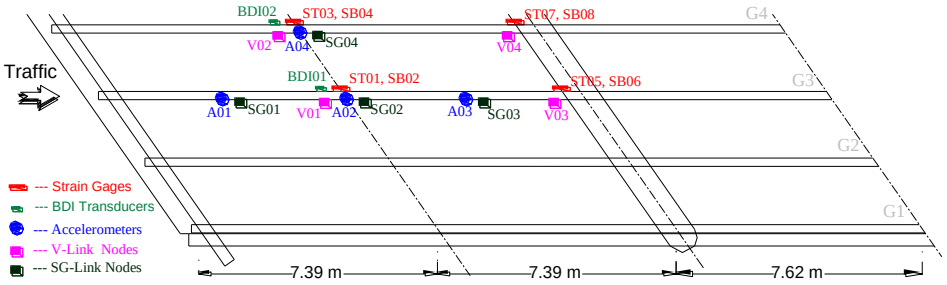


(a) Instrumentation plan

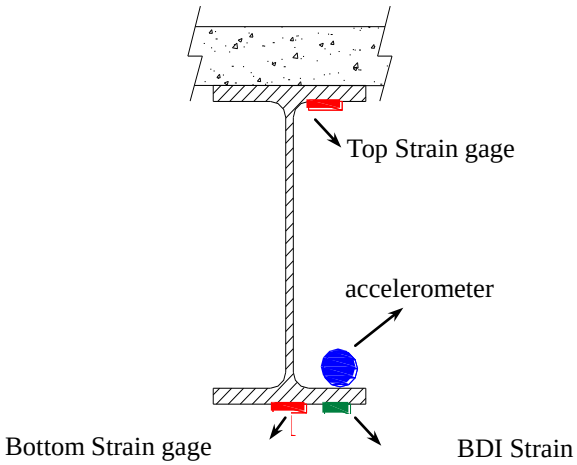


(b) Typical instrumentation configuration on girder at mid-span

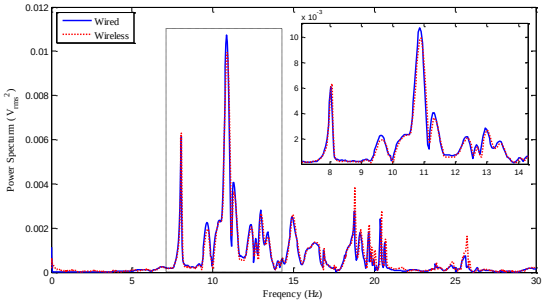


(c) Sensors installed on bottom flange of steel girder

Fig. 9 Layout of instrumentation on Evansville Bridge Superstructure for Load Testing

Strain gages and transducers were installed on two of the seven girders along the first span as shown in Fig. 9. Strain gage pairs were installed at four locations on each girder, to measure strain response both on the top and bottom flanges at each location. To confirm the strain results, two additional BDI strain transducers were clamped on the bottom flanges at mid-span on these two girders, parallel with strain gage pairs. Three accelerometers were installed on girder No.3 at ¼

span, ½ span and ¾ span respectively. One additional accelerometer was mounted on girder No.4. Four SG-Link nodes were connected to the four accelerometers respectively through signal conditioning boards. Four V-Link nodes were connected with strain gage pairs and BDI transducers at four locations. The sampling rate was set at 256 Hz for a recording time duration was 50 seconds.

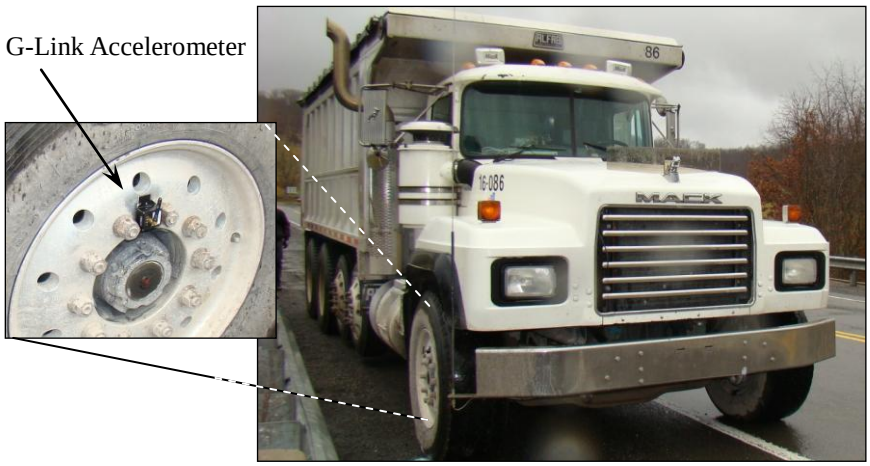


Fig. 10 Instrumented test truck

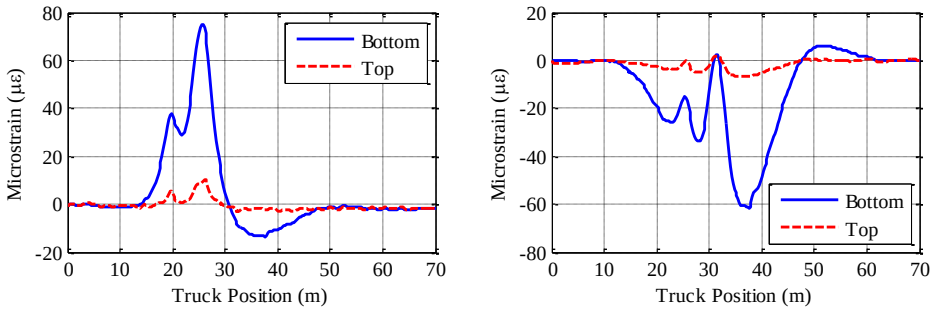


(a) At Mid-Span (b) At Pier

Fig. 11 Strain Response on girder No.3 due to Static Load

A fully loaded three-axle dump truck was used to apply static as well as dynamic loading on the bridge. The gross weight of the test truck was 304 KN (68.22 kips). The front axle weighed 92 KN (20.68 kips), while each of the two rear ones weighed 106 KN (23.77 kips). The test truck rolled across the bridge following a designated path on the instrumented eastbound lane, where the outside wheel was at 0.45 m from the bridge center line. Fig. 10 illustrates the instrumented loading truck. A starting point for measuring the truck position was assigned where the front axle was 10 m away from the bridge end. The static test was performed by having the truck crossing the bridge with a crawl speed (~8 km/h) when no traffic was present. This took less than 50 seconds.

Data from all sensors were recorded simultaneously with a sampling rate of 256 Hz. In total, six runs were carried out; strain and acceleration responses were recorded and averaged for analysis.

The dynamic test was carried out 3 times by driving the test truck across the bridge at regular speed (55 km/h) following the same wheel path, also in absence of other traffic. Fig. 11 illustrate samples of data collected from the static test in the truck-position domain. Fig. 12 shows the time domain and the frequency domain signals of the acceleration recoded at mid-span on Girder No.4.

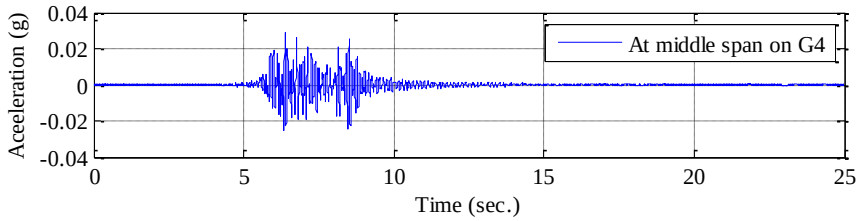


(a) Time domain

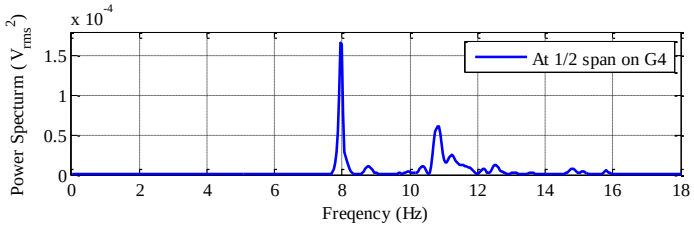


(a) Frequency Domain

Fig. 12 Acceleration measurements on Evansville Bridge through Dynamic Test

## 7. Finite element model study

In an effort to optimize the number of sensors mounted on the bridge superstructure, only the 2 interior main girders carrying the East bound lane have been instrumented. In this case, the load distribution factor for the seven girders, which is required for the calculations of the rating factor were determined through a finite element model study. For this purpose, a finite element model of the entire bridge was conducted using SAP2000 software, and its results validated through a comparison with the recorded measurements from the field test. The model used shell elements for the bridge deck, girders, and piers. Table 2 lists the boundary conditions adopted for the model supports while the material properties assigned to the model are shown in Table 3. The spring action on the supports of the abutment walls take into consideration the passive force of the earth pressure and the effect of the bridge $55^{o}$ skewed angle. Fig. 13 illustrates the finite element model along with a comparison of calculated bending moments from the field test data, and those collected from the finite element model on both Girders No. 3 and No. 4. As can be seen, the finite element model response to the moving truck load was in good agreement with measured data collected from the field test. The load distribution factors as calculated from the finite element model results are listed in Table 4. As can been seen from Table 4, when the south lane is loaded with the test truck, Girder No.3 is the critical member and carries 30.2% of the truck moment. When both lanes are loaded, Girder No.4 becomes the critical one and carries 53.2% of the truck

moment. Such results validate the assumption that Girders No. 3 and No. 4 were the critical ones to carry the truck load, thus were instrumented.

Table 2 Boundary conditions and degrees of freedom at bridge supports

| Supports | Translation | | | Rotation | | |
|---|---|---|---|---|---|---|
| | x | y | z | x | y | z |
| Abutment 1 | Spring 62686 KN/m | Spring 43893 KN/m | x | x | ✓ | ✓ |
| Pier 1 | x | x | x | x | ✓ | x |
| Pier 2 | ✓ | x | x | x | ✓ | x |
| Abutment 2 | Spring 62686 KN/m | Spring 43893 KN/m | x | x | ✓ | ✓ |

x: Fixed ✓: Free

Table 3 Material properties assigned to finite element model

| Properties | Steel | Concrete |
|---|---|---|
| Modulus of Elasticity (GPa) | 199.995 | 30.23 |
| Poisson's Ratio | 0.3 | 0.24 |
| Density (kg/m$^3$) | 7750.4 | 2395.7 |
| Coefficient of Thermal Expansion (/$^o$C) | 1.22x10$^{-5}$ | 1.126x10$^{-5}$ |

Table 4 Load distribution factors of steel girders calculated from finite element model study

| Girder No. | Lane 1 Loaded (%) | Lane 2 Loaded (%) | 2 Lanes Loaded (%) |
|---|---|---|---|
| G1 | 6.9 | 1.0 | 7.9 |
| G2 | 16.3 | 5.7 | 22 |
| G3 | 30.2 | 13.3 | 43.5 |
| G4 | 26.6 | 26.6 | 53.2 |
| G5 | 13.3 | 30.2 | 43.5 |
| G6 | 5.7 | 16.3 | 22 |
| G7 | 1.0 | 6.9 | 7.9 |
| Total | 100 | 100 | 200 |

## 8. Field test rating factors

The maximum theoretical moment ($M$) on Girder No. 4 produced by the test truck on the bridge was calculated to be

$$M = 616.0 \text{ KN.m}$$

When both lanes are loaded, this bending moment ($M_m$) can be calculated by multiplying ($M$) with the load distribution factor ($LDF$) taken from Table 4

$$M_m = M \times LDF = 616 \times 53.2\% = 327.7\text{KN.m.} \quad (9)$$

Identifying the factors from LRFR manual, $K_a$ = 0.998, $K_b$ = 0.64, the rating factor $K$ can be

computed to be: $K$ = 1.64. Thus, the bridge rating factors from the load test can be determined by multiplying the theoretical rating factors in Table 1 by 1.64.

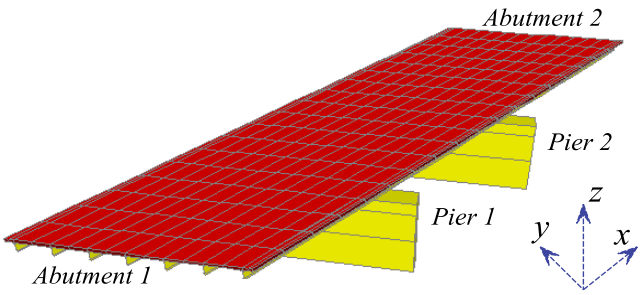


(a) Finite Element Model (FEM) Geometry

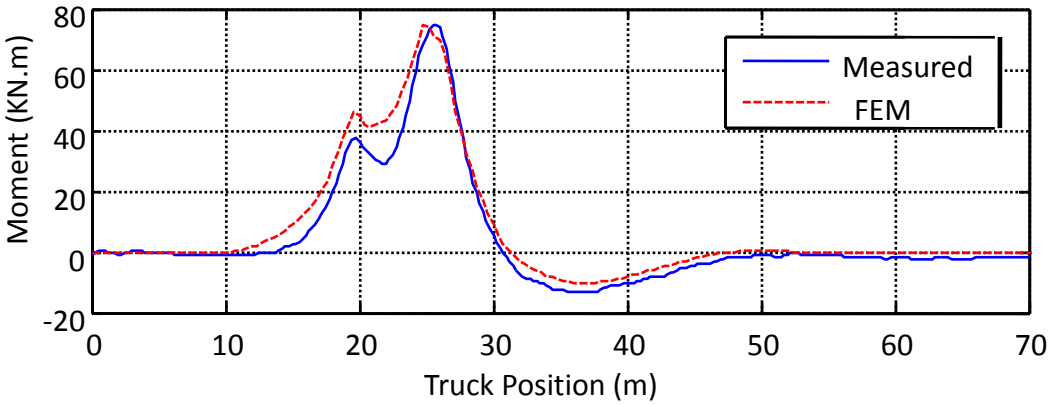


(b) Comparison of FEM vs Field Test Bending Moments on Girder No.3 at Mid-Span

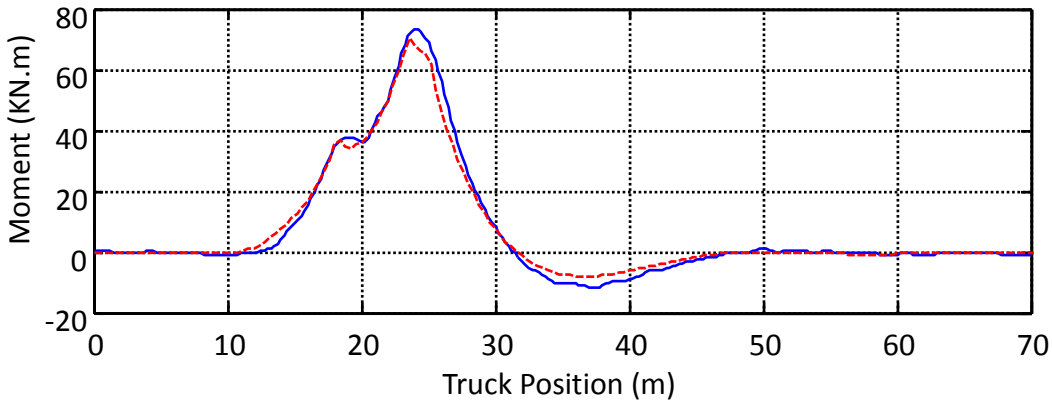


(c) Comparison of FEM vs Field Test Bending Moments on Girder No.4 at Mid-Span

Fig. 13 Finite Element Model Study of Evansville Bridge

The load test results were again verified by conducting a second test on the same bridge about

one month later. The test truck at this time had a gross weight of 300 KN and axle configurations of 80 KN, 110 KN, and 110 KN for the front and rear axles respectively. The exact instrumentation plan and test procedures were followed as for the previous one. In this test, the distance between the outside wheel path and the bridge center line was 1.06 m. In this case, the maximum strains measured on the steel girder varied by 10% compared to that recorded from the first load test. When both lanes were loaded, Girder No.4 carried 49.4% of the truck moment. Following the same procedures, the adjustment factor *K* was calculated to be 1.69. The calculated adjustment factor varied by only 3% compared to that calculated from the first loading test.

## 9. Conclusions

In this study, a wireless sensory system for bridge load testing and rating is presented. The system provides a reliable and low-cost technology for structural evaluation of highway bridges using LRFR procedures. The wireless sensory system includes wireless strain sensors, wireless accelerometers and a wireless vehicle position indicator for monitoring loading truck positions during load testing. The vehicle position indicator uses a tri-axial accelerometer node that is mounted on the test vehicle hub. The sinusoidal acceleration signal recorded from the rotating motion of the vehicle wheel is translated into a linear position of the test vehicle referenced from a predetermined starting point. Along with the wireless platform, software is developed in Matlab code following the LRFR procedures for calculating both theoretical and field ratings. An example of conducting a load rating test is presented where the sensory system was successfully deployed on the Evansville Bridge in West Virginia and was used to conduct a field load rating test after identifying the theoretical bridge rating according to LRFR. A finite element study on the test bridge was conducted to optimize the number of sensors, and confirmed that only 2 girders of the bridge needed to be instrumented to provide the necessary rating data. A second rating test was conducted on the same bridge using the same instrumentation and proved to have good repeatable results with only 3% variation in the field rating adjustment factor.

## References

AASHTO Guide Manual for Condition Evaluation and Load and Resistance Factor Rating (LRFR) of Highway Bridges (2003), *American association of state highway and transportation officials*, Washington, D.C.

Chajes, M.J., Mertz, D.R. and Commander B. (1997), "Experimental load rating of a posted bridge", *J. Bridge Eng.*, **2**(1), 1-10.

Chase, S. (2001), "The role of smart structures in managing an aging highway infrastructure", Keynote *Presentation in SPIE 8th Annual International Symposium on Smart Structures and Materials*, Newport Beach, CA, USA, March 4-8.

Chong, C.Y. and Kumar, S.P. (2003), "Sensor networks: evolution, opportunities, and challenges", *P. IEEE*, **91**(8), 1247-1256.

Flouri, K., Saukh, O., Sauter, R., Jalsan, K.E., Bischoff, R., Meyer, J. and Feltrin, G. (2012), "A versatile software architecture for civil structure monitoring with wireless sensor networks", *Smart Struct. Syst.*, **10** (3), 209-228.

Hoover, D.P., Bilbao, A. and Rice, J.A. (2012), "WiSeMote: a novel high fidelity wireless sensor network for structural health monitoring", *Smart Struct. Syst.*, **10**(3), 271-298.

Kim, J.T., Ho, D.D., Nguyen K.D., Hong D.S., Shin, S.W., Yun, C.B. and Shinozuka, M. (2013), "System identification of a cable-stayed bridge using vibration responses measured by a wireless sensor network", *Smart Struct. Syst.*, **11**(5), 533-553.

Jo, H., Park, J.W., Spencer, B.F. Jr. and Jung, H.J. (2013), "Develoment of high-sensitivity wireless strain sensor for structural health monitoring" , *Smart Struct. Syst.*, **11** (5), 477-496.

Lichtenstein, A.G. (1998), *Manual for bridge rating through load testing*, Research Results Digest, No. 234, National Cooperative Highway Research Program, Washington, D.C.

Lin, H.R., Chen, C.S., Chen, P.Y., Tsai, F.J., Huang, J.D., Li, J.F., Lin, C.T. and Wu, W.J. (2010), "Design of wireless sensor network and its application for structural health monitoring of cable-stayed bridge", *Smart Struct. Syst*., **6**(8), 939-951.

Luo, Y. (2010), "Wireless sensing system for load testing and rating of highway bridges", Ph.D. Dissertation, Department of Mechanical and Aerospace, West Virginia University, Morgantown, WV.

Lynch, J.P. and Loh, K.J. (2006), "A summary review of wireless sensors and sensor networks for structural health monitoring", *Shock Vib.*, **38**(2), 91-128.

Ni, Y.Q., Li, B., Lam, K.H., Zhu, D.P., Wang, Y., Lynch, J.P. and Law, K.H. (2011), "In-construction vibration monitoring of a super-tall structure using a long-range wireless sensing system", *Smart Struct. Syst*., **7**(2), 83-102.

Phares, B.M., Wipf T.J., Klaber, F.W., Abu-Hawash, A. and Neubauer, S.(2005), "Implementation of physical testing for typical bridge load and superload rating", *Transportation Research Record: Journal of the Transportation Research Board (CD-11S)*: pp. 159-167.

Phares, B.M., Wipf, T.J., Klaber, F.W. and Abu-Hawash, A. (2003), "Bridge load rating using physical testing", *Proceedings of the 2003 Mid-Continent Transportation Research Symposium*, Ames, Iowa, August 2003.

Selesnick, I.W. (2004), "The double density dual-tree discrete wavelet transforms", *IEEE T. Signal Proces*., **52** (5).

Straser, E.G. and Kiremidjian, A.S. (1998), *A modular, wireless damage monitoring system for structures*, Report No. 128, John A. Blume Earthquake Eng. Ctr., Stanford University, Stanford, CA.

Yuan, S., Wang, Z., Qiu, L., Wang, Y. and Liu, M. (2013), "A multi-radio sink node designed for wireless SHM applications", *Smart Struct. Syst*., **11**(3), 261-282.

Washer, G. and Fuchs, P. (1998), "Better load ratings through nondestructive evaluation", *Public Roads*, **62**(3), 41-44.

*CC*